

# ***New MR Imaging Techniques in The Diagnosis of Orbital Tumors***

*Essay submitted for the partial fulfillment of  
M.S. degree in Radiodiagnosis*

*By*

**Hany Mohamed Abbas Hamoda**

**M.B.B.Ch**

Under supervision of

***Dr. Naglaa Mohamed Abdel Razeq***

***Assistant Professor of Radiology***

***Cairo University***

***Dr. Ramy Edward Asaad***

***Lecturer of Radiology***

***Cairo University***

***Faculty of Medicine***

***Cairo University***

**2010**

## **Abstract**

Magnetic resonance spectroscopy applications in neuro-ophthalmology include differentiating ischemic, neoplastic, demyelinating, radiation necrosis, inflammatory, and mitochondrial disorders affecting the visual pathway.

Key word:

MR

Diagnosis

Tumors

# Acknowledgement

*First of all, thanks to Allah. After that I wish to express my deep thanks to Prof. Dr. Naglaa Mohamed Abdel Razeq, Assistant Professor of Radiology, Cairo University to provide me with the initial motive which aroused my interest in this work and for making a substantial contribution to this outcome.*

*Also, I want to express my deep and great thanks to Dr. Ramy Edward Asaad, lecturer of Radiology, Cairo University for his valuable help & guidance.*

## CONTENT

Introduction	I
Abbreviations	IV
List of figures	V
Anatomy	1
PATHOLOGY AND IMAGING FEATURES	28
-Intraconal neoplasms	31
-Extraconal neoplasms	46
-Extraocular muscle enlargement	62
-Ocular neoplasms	62
-Lacrimal gland neoplasms	66
NEW MR IMAGING TECHNIQUES	70
-Kinetic MRI of the orbit	70
-Three dimensional high resolution MRI	75
-Non invasive dynamic MRA	82
-MR Diffusion	88
-MR Spectroscopy	94
Summary	98
References	101

---

## INTRODUCTION AND AIM OF THE WORK

---

A variety of tumors can involve the orbit. Cystic tumors, vasculogenic tumors, peripheral nerve lesions, optic nerve and meningeal tumors, fibrocytic lesions, osseous and fibro-osseous tumors, cartilaginous tumors, lipocytic and myxoid lesions, myogenic tumors, lacrimal gland lesions, primary melanocytic lesions, metastatic tumors, lymphoma and leukemia lesions, secondary orbital tumors, histiocytic lesions are known orbital neoplasms with malignancies being common in older patients because of the higher incidence of lymphoma and metastasis in the elderly. **(Shields et al., 2004)**

Magnetic resonance imaging (MRI), computed tomography (CT) and orbital ultrasound form the main stay in orbital imaging techniques. **(Fischbein et al., 2002)**

MRI is preferred for orbital imaging because its lack of ionizing radiation, fine delineation of detail and excellent demonstration of intracranial pathology. **(Ortiz and Flores, 1998)**

CT is reserved for evaluation of trauma, foreign body, lesion that may calcify orbital cellulitis and orbital disease secondary to sinus disease. **(Lee et al, 2004)**

Head surface coils and smaller coils with thin section fat suppressed T2 or short time inversion recovery (STIR) coronal images are required to study the orbits optimally. Sagittal, coronal, and axial T1 weighted images and T2 weighted scans with pre-contrast fat suppression in at least one plane, usually coronal and post-contrast axial and coronal planes may be supplemented to clearly show an optic nerve sheath lesion and intraorbital inflammation. **(Rizzo et al., 2002)**

---

---

Enhanced T1 weighted images are useful for neoplastic, inflammatory, ischemic, vascular, demyelinating and infiltrative processes. (**Ortiz and Flores, 1998**)

For evaluating the intracranial extent of a lesion, whole-brain sections are added when indicated including axial dual-echo spin-echo T2-weighted and post-gadolinium axial and sagittal T1-weighted images. Ultrathin-section 3-dimensional fast spin echo (3-D FSE) T2-weighted imaging is a new MRI technique that offers superior resolution of intraocular and orbital structures compared with conventional MRI. (**Fischbein et al., 2002**)

Magnetic resonance angiography (MRA) and venography can provide noninvasive static views of the orbital vasculature and some limited indirect information about blood flow. Dynamic MRA in the form of time-resolved imaging of contrast kinetics (TRICKS) is a newly available imaging modality with great potential for improving the evaluation and management of patients with complex orbital tumors. (**Kahana et al., 2007**)

Advanced quantitative structural MR imaging techniques include magnetization transfer imaging, diffusion weighted imaging and perfusion weighted imaging, their applications include evaluation of hyperacute ischemia, inflammatory, degenerative and neoplastic lesions. Magnetic resonance spectroscopy MRS is based on detecting various proton MR spectra with applications including differentiation of ischemic, neoplastic, demyelinating, radiation necrosis, inflammatory and mitochondrial disorders affecting visual pathway. MRS has also used anecdotally in evaluating intraorbital tumors. (**Lee et al., 2004**)

An integrated MR imaging-based strategy including these studies with conventional MRI can increase the accuracy, sensitivity and specificity for discrimination of neoplastic from non neoplastic lesions, further more it can

---

---

discriminate low grade neoplasms from high grade neoplasms and lymphoma lesions especially with associated brain lesions. (**AL-Okaili et al., 2007**)

The aim of that work is to evaluate the role of new MR imaging techniques in diagnosis and staging of orbital tumors as well as their role in operative and therapeutic planning and follow up.

## LIST OF ABBREVIATIONS

ADC= Apparent diffusion coefficient  
AML= Acute myelogenous leukemia  
CN= Cranial nerve  
CNS= Central nervous system  
CT= Computed tomography  
DCM= Dynamic color mapping  
ENB= Esthesioneuroblastoma  
FLAIR= Fluid-attenuated inversion recovery  
FS= fat suppression  
FSE= Fast spin echo  
Gd – DTPA= Gadolinium diethylenetriamine penta-acetic acid  
IR= inversion recovery  
MRA= Magnetic resonance arteriography  
MRI= Magnetic resonance imaging  
MRS= Magnetic resonance spectroscopy  
MRV= Magnetic resonance venography  
NF= Neurofibromatosis  
OCT= Optical coherence tomography  
ONB= Olfactory neuroblastoma  
ONSM= optic nerve sheath meningioma  
PD= Proton density  
PNETs= Primitive neuroectodermal tumors  
RB= Retinoblastoma  
SE= Spin echo  
STIR= short-tau inversion-recovery  
TE= Echo time  
TR= Time repetition  
TRICKS= Time-resolved imaging of contrast kinetics  
2D= two dimensional  
3D= three dimensional

---



## List of Figures

<b>Figure number</b>	<b>Contents</b>
<b>Figure (1)</b>	Diagram of the bony orbit
<b>Figure (2)</b>	MRI of the orbit showing hypointense bone in all pulse sequences.
<b>Figure (3)</b>	CT of the orbit in bone window.
<b>Figure (4)</b>	Diagram demonstrating a section through the right eye.
<b>Figure (5)</b>	Optic nerve shown in MRI, CT, skull bone
<b>Figure (6)</b>	Diagram of the arterial supply of the orbit
<b>Figure (7)</b>	Diagram of the venous drainage of the orbit
<b>Figure (8)</b>	Extraorbital portion of the ophthalmic artery in MRI
<b>Figure (9)</b>	Superior ophthalmic vein in sagittal MRI.
<b>Figure (10)</b>	Diagram of extraocular muscles.
<b>Figure (11)</b>	Extraocular muscles demonstrated in coronal MRI.
<b>Figure (12)</b>	Contrast-enhanced fat suppressed MRI showing intense enhancement of extraocular muscles.
<b>Figure (13)</b>	Diagram of lacrimal apparatus.
<b>Figure (14)</b>	MRI showing lacrimal gland in supero-lateral portion of the orbit.
<b>Figure (15)</b>	The globe in diagram.
<b>Figure (16)</b>	The globe in axial T2W1 MRI.
<b>Figure (17)</b>	CT scout view of axial and Coronal imaging protocols.
<b>Figure (18)</b>	Diagram of the orbital compartments.

<b>Figure (19)</b>	MRI of optic nerve glioma in 6-year old girl.
<b>Figure (20)</b>	MRI of optic glioma in 46-year-old woman.
<b>Figure (21)</b>	CT of calcified right sphenoid wing meningioma.
<b>Figure (22)</b>	MRI of calcified optic nerve sheath meningioma.
<b>Figure (23)</b>	MRI of orbital meningeal metastasis of NH-lymphoma.
<b>Figure (24)</b>	CT of orbital leukemic chloroma.
<b>Figure (25)</b>	MRI of orbital leptomeningeal metastasis.
<b>Figure (26)</b>	MRI of orbital cavernous hemangioma.
<b>Figure (27)</b>	CT of orbital varices.
<b>Figure (28)</b>	Multiple intraorbital neurofibromas in CT and MRI.
<b>Figure (29)</b>	CT of orbital neurinoma.
<b>Figure (30)</b>	CT of orbital juvenile capillary hemangioma.
<b>Figure (31)</b>	CT of orbital lymphangioma
<b>Figure (32)</b>	MRI of orbital lymphangioma
<b>Figure (33)</b>	MRI of orbital rhabdomyosarcoma.
<b>Figure (34)</b>	Right maxillary antrum carcinoma with orbital extension (CT).
<b>Figure (35)</b>	carcinoma of the left maxillary sinus with orbital extension (MRI).
<b>Figure (36)</b>	CT of neuroblastoma.
<b>Figure (37)</b>	MRI showing orbital extension of esthesioneuroblastoma.
<b>Figure (38)</b>	Meningioma of the right sphenoid wing (CT bone window).
<b>Figure (39)</b>	Osteoma of the right ethmoid bone in CT and MRI.

<b>Figure (40)</b>	CT of Fibrous dysplasia.
<b>Figure (41)</b>	Aneurysmal bone cyst associated with fibrous dysplasia in CT.
<b>Figure (42)</b>	Orbital metastasis of breast carcinoma in CT.
<b>Figure (43)</b>	MRI showing metastatic neuroblastoma.
<b>Figure (44)</b>	MRI showing uveal metastasis from lung cancer.
<b>Figure (45)</b>	CT (postcontrast) of bilateral retinoblastoma.
<b>Figure (46)</b>	MRI showing bilateral retinoblastoma.
<b>Figure (47)</b>	MRI showing choroidal melanoma
<b>Figure (48)</b>	CT of orbital lymphoma.
<b>Figure (49)</b>	MRI of Lacrimal gland dermoid.
<b>Figure (50)</b>	Normal orbital soft tissue motion obtained by MRI-DCM in normal subject.
<b>Figure (51)</b>	Localization of orbital mass with MRI-DCM
<b>Figure (52)</b>	MRI-DCM in the measurement of soft tissue motion after enucleation.
<b>Figure (53)</b>	Pre-treatment and post-treatment appearance of retinoblastoma in conventional MRI and 3-D FSE T2-weighted image.
<b>Figure (54)</b>	Retinoblastoma (Rb) with radiation-associated cataract in conventional MRI and 3-D FSE T2-

	weighted image.
<b>Figure (55)</b>	Lymphoma in conventional MRI and 3-D FSE T2-weighted image.
<b>Figure (56)</b>	Probable venolymphatic malformation in conventional MRI and 3-D FSE T2-weighted image.
<b>Figure (57)</b>	Ciliary body melanoma in conventional MRI and 3-D FSE T2-weighted image.
<b>Figure (58)</b>	Hemangiopericytoma in (TRICKS MRA).
<b>Figure (59)</b>	Orbitocutaneous arteriovenous malformation in (TRICKS MRA).
<b>Figure (60)</b>	Orbital varix in (TRICKS MRA).
<b>Figure (61)</b>	Cavernous hemangioma. In (TRICKS MRA).
<b>Figure (62)</b>	Orbital lymphoma with conventional MRI and DW1 images.
<b>Figure (63)</b>	A profile of the demonstration of normal optic nerve using DTI.
<b>Figure (64)</b>	Demonstration of normal optic nerve using DTI.
<b>Figure (65)</b>	Demonstration of a case of meningioma using DTI.
<b>Figure (66)</b>	Glioblastoma of the optic pathway (MR Flair).
<b>Figure (67)</b>	Glioblastoma of the optic pathway (MR T2W).
<b>Figure (68)</b>	Glioblastoma of the optic pathway (MR post contrast T1).

---

---

<b>Figure (69)</b>	Glioblastoma of the optic pathway (MR spectroscopy).
<b>Figure (70)</b>	Multiple sclerosis (MR T2W).
<b>Figure (71)</b>	Comparison of normal spectra and that of low grade glioma.

---

---

---

---

## ANATOMY

### Osteology

The orbit functions to protect, support, and maximize function of the eye. The orbit is shaped as a quadrilateral pyramid with its base in plane with the orbital rim. Seven bones conjoin to form the orbital structure. The orbital process of the frontal bone and the lesser wing of the sphenoid form the orbital roof. The orbital plate of the maxilla joins the orbital plate of the zygoma and the orbital plate of the palatine bones to form the floor. Medially, the orbital wall consists of the frontal process of the maxilla, the lacrimal bone, the sphenoid, and the thin lamina papyracea of the ethmoid. The lateral wall is formed by the lesser and greater wings of the sphenoid and the zygoma (figure 1). **(Petruzzi et al., 2008)**

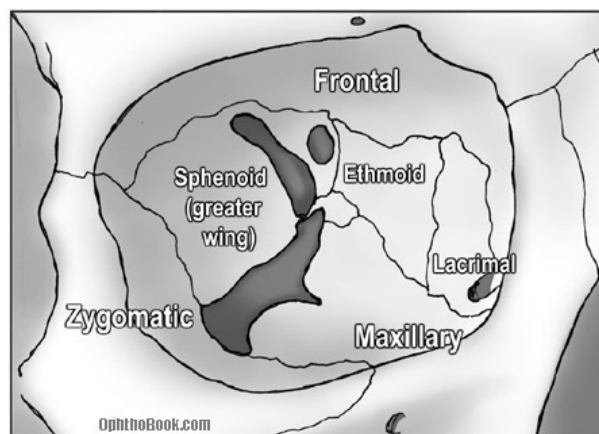


**Fig.(1):** Diagram of the right orbit shows the 7 bones that contribute to its structure. **(Layfield et al., 2006)**

The arc from medial to lateral wall in each orbit is 45°. Lines dropped through a central anterior-to-posterior axis of each orbit bisect at a 45° angle. The floor is two-thirds the depth of the orbit. The average dimensions of the orbit are as follows:

- Height of orbital margin - 40 mm
- Width of orbital margin - 35 mm
- Depth of orbit - 40-50 mm
- Interorbital distance - 25 mm
- Volume of orbit - 30 cm<sup>3</sup> (**Petruzzi et al., 2008**)

The superficial bony orbit is defined by the orbital margin, which is rectangular with rounded corners. The margin is discontinuous at the lacrimal fossa. The supraorbital notch is within the supraorbital rim and is closed to form the supraorbital foramen in 25% of individuals. The supratrochlear notch is medial to the supraorbital notch. The trochlea is a cartilaginous ring that supports the superior oblique muscle. The trochlea attaches to the periorbita within the fovea trochlearis along the superior-medial orbit. The infraorbital foramen is located 10 mm inferior to the zygomaticomaxillary suture. Laterally, the orbital rim is marked by the Whitnall tubercle, which is 10 mm inferior to the zygomaticofrontal suture. The tubercle is the site of attachment of the lateral canthal tendon. (**Petruzzi et al., 2008**)